

Article

An In Situ Study on Nanozyme Performance to Optimize Nanozyme-Strip for A β Detection

Yaying Luo ^{1,2}, Haiming Luo ³ , Sijia Zou ^{2,4}, Jing Jiang ², Demin Duan ², Lei Chen ² and Lizeng Gao ^{2,*} 

¹ School of Life Sciences, Division of Life Sciences and Medicine, University of Science and Technology of China, Hefei 230026, China

² CAS Engineering Laboratory for Nanozyme, Institute of Biophysics, Chinese Academy of Sciences, Beijing 100101, China

³ MoE Key Laboratory for Biomedical Photonics, School of Engineering Sciences, Huazhong University of Science and Technology, Wuhan 430074, China

⁴ School of Basic Medical Sciences, Southwest Medical University, Luzhou 646000, China

* Correspondence: gaolizeng@ibp.ac.cn

Abstract: The nanozyme-strip is a novel POCT technology which is different from the conventional colloidal gold strip. It primarily utilizes the catalytic activity of nanozyme to achieve a high-sensitivity detection of target by amplifying the detection signal. However, previous research has chiefly focused on optimizing nanozyme-strip from the perspective of increasing nanozyme activity, little is known about other physicochemical factors. In this work, three sizes of Fe₃O₄ nanozyme and three sizes of CoFe₂O₄ nanozyme were used to investigate the key factors of nanozyme-strip for optimizing and improving its detection performance. We found that three sizes of Fe₃O₄ nanozyme all gather at the bottom of the nitrocellulose (NC) membrane, and three sizes of CoFe₂O₄ nanozyme migrate smoothly on the NC membrane, respectively. After color development, the surface of NC membranes distributed with CoFe₂O₄ peroxidase nanozymes had significant color change. Experimental results show that CoFe₂O₄ nanozymes had better dispersity than Fe₃O₄ nanozymes in an aqueous solution. We observed that CoFe₂O₄ nanozymes with smaller particle size migrated to the middle of the NC membrane with a higher number of particles. According to the results above, 55 ± 6 nm CoFe₂O₄ nanozyme was selected to prepare the nanozyme probe and achieved a highly sensitive detection of A β 42Os on the nanozyme-strip. These results suggest that nanozyme should be comprehensively evaluated in its dispersity, the migration on NC membrane, and the peroxidase-like activity to determine whether it can be applied to nanozyme-strip.

Keywords: nanozyme-strip; peroxidase-like activity; NC membrane; in situ characterization; A β detection



Citation: Luo, Y.; Luo, H.; Zou, S.; Jiang, J.; Duan, D.; Chen, L.; Gao, L. An In Situ Study on Nanozyme Performance to Optimize Nanozyme-Strip for A β Detection. *Sensors* **2023**, *23*, 3414. <https://doi.org/10.3390/s23073414>

Academic Editor: Chengzhou Zhu

Received: 17 February 2023

Revised: 18 March 2023

Accepted: 22 March 2023

Published: 24 March 2023



Copyright: © 2023 by the authors. Licensee MDPI, Basel, Switzerland. This article is an open access article distributed under the terms and conditions of the Creative Commons Attribution (CC BY) license (<https://creativecommons.org/licenses/by/4.0/>).

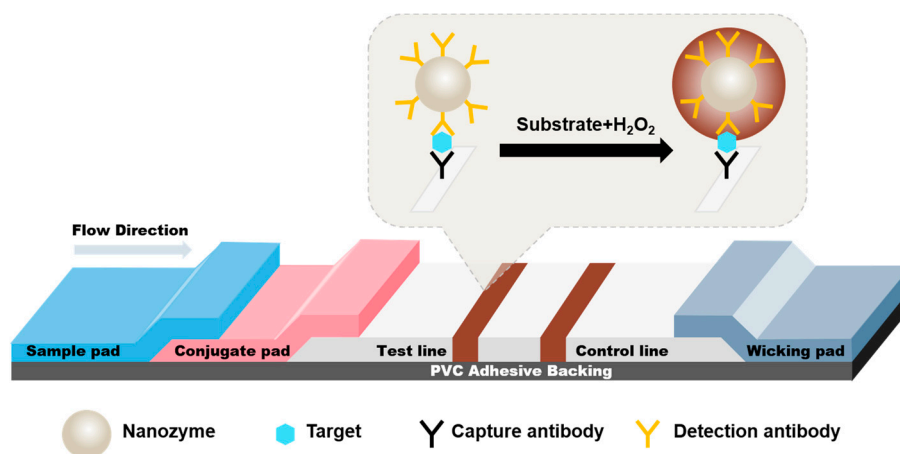
1. Introduction

Lateral flow immunoassay (LFIA) is a paper-based point-of-care testing (POCT) diagnostic tool, also known as test strips, which has been widely used for rapid detection and early screening of many diseases [1–4]. Compared with laboratory tests such as enzyme-linked immunosorbent assay (ELISA) and polymerase chain reaction (PCR), LFIA does not require automated instruments and professional testing personnel, and has the advantages of simple operation, rapid detection, and low cost. LFIA has been applied in many fields such as disease, agriculture, food, and so on. The most established LFIA is the colloidal gold nanoparticle-based paper strip (AuNP-strip) [5,6]. However, since the detection sensitivity of the AuNP-strip is significantly lower than those of laboratory assays, the reference value of its detection results is greatly reduced, which limits its application in disease monitoring. Upon on the above problems, many researchers have introduced nanozymes into paper strips in recent years [7–11] to replace the colloidal gold nanoparticles and developed nanozyme-strip with high sensitivity.

Nanozymes are a class of artificial nanomaterials with similar catalytic activity to natural enzymes [12–15], which are classified into four major categories based on their natural enzyme-like activities: oxidoreductases, hydrolases, polymerases, and isomerases [14]. Nanozymes possess superiorities due to their low cost, high stability, and easy preparation. Nowadays, nanozyme-strips mainly utilize the higher peroxidase (POD) activity of peroxidase nanozymes to generate colored products by catalyzing the oxidation of substrates, and accumulate in the detection zone to amplify the detection signal and enhance the detection sensitivity. Since the rapid detection of the Ebola virus using nanozyme-strip was first published by Yan teams in 2015 [16], many works on nanozyme-strip have been published [11,17,18]. The detection limit of the paper strip for procalcitonin reached 0.5 pg/mL, and its sensitivity was 2280-fold higher than that of the AuNP-strip [17].

Alzheimer's disease is an irreversible neurodegenerative disease most common in the elderly. Amyloid β ($A\beta$) is considered to be the earliest detectable preclinical biomarker associated with the pathogenesis of AD [19]. $A\beta$ consists of 38–43 amino acid residues derived from amyloid precursor protein that is sequentially cleaved by β - and γ -secretases, of which $A\beta_{42}$ is the most neurotoxic [20]. Currently, abnormal $A\beta_{42}$ levels can be detected in CSF and $A\beta$ -PET neuroimaging [21,22]. However, these methods are difficult to be widely used because of high testing cost, invasiveness, and equipment requirements. It has been reported that the level of $A\beta_{42}$ oligomers ($A\beta_{42}Os$) reflects the level of $A\beta_{42}O$ in CSF and is highly correlated with the progression of AD, and thus has the potential to diagnose AD [23]. Based on the above, we are determined to take advantage of nanozyme-strips for rapid detection of $A\beta_{42}Os$.

The nitrocellulose (NC) membrane is the carrier for the immunoreaction of nanozyme-strip [24]. After the detected target is specifically bound to the nanozyme probe as an antigen, it migrates forward on the NC membrane in the form of a complex. When it moves to the area where the capture antibody is immobilized, the complex is trapped by the antigen-antibody reaction. Here, the detection is finally realized by forming a test line (T line) and a quality control line (C line) through color development (Scheme 1). As a result, the migration state of the nanozyme probe on the NC membrane is crucial to the final detection effect. However, the current design of nanozyme-strip focuses on how to improve the peroxidase-like activity of the nanozyme probe, while its flow state on the NC membrane has not been systematically studied. Factors such as size, morphology, and dispersion of nanozymes may affect their migration on the NC membrane and have a poor impact on the detection results.



Scheme 1. The principle and structure of a nanozyme-strip.

In this article, $CoFe_2O_4$ and Fe_3O_4 nanozymes with different particle sizes synthesized in the laboratory were used to explore the factors affecting the migration of nanozyme probes on test strips, and the most suitable nanozyme was selected to prepare detection probes. By visualizing the distribution of nanozymes on NC membranes, we found that

well-dispersed nanozymes do not aggregate during migration on NC membranes; the smaller the particle size, the better their uniform distribution on NC membranes. The POD activity of a nanozyme affects the color development of a nanozyme on the NC membrane. Finally, we comprehensively selected the 55 ± 6 nm CoFe_2O_4 peroxide nanozyme which had the best performance on the NC membrane for the preparation of nanozyme probes, and successfully detected $\text{A}\beta_{42}$ oligomers ($\text{A}\beta_{42}\text{Os}$), the blood marker of Alzheimer's disease (AD) on the nanozyme-strip [25].

2. Materials and Methods

2.1. Reagents and Chemicals

Ferric chloride ($\text{FeCl}_3 \cdot 6\text{H}_2\text{O}$), cobalt chloride hexahydrate ($\text{CoCl}_2 \cdot 6\text{H}_2\text{O}$), ethylene glycol, diethylene glycol, 3,3',5,5'-tetramethylbenzidine (TMB), sodium acetate trihydrate ($\text{NaAc} \cdot 3\text{H}_2\text{O}$), and dimethyl sulfoxide (DMSO) were purchased from Sigma (Los Angeles, CA, USA). A nitrocellulose membrane was brought from Sartorius (Göttingen, Germany). Detachable 96-well plate, and bovine serum albumin (BSA) were purchased from Lablead Biotechnology Co., Ltd. (Beijing, China); 30% H_2O_2 was purchased from Sinopharm Chemical Reagent Co., Ltd. (Shanghai, China). The DAB color development kit was purchased from ZSGB-Bio (Beijing, China). Anti-beta Amyloid antibody was brought from Abcam (Cambridge, UK). The 1F12 monoclonal antibody was supplied by courtesy of Prof Haiming Luo's Lab in the Huazhong University of Science and Technology (Wuhan, China).

2.2. Instrumentation

An ultraviolet (UV) spectrophotometer (Beckham Coulter, Brea, CA, USA) was utilized to measure the absorption of TMB working solution with nanozymes at 652 nm. Particle size and Zeta Potential Analyzer (Brookhaven, New York, NY, USA) was applied to measure the value of Zeta potential and PDI. X-ray powder diffractometer (Bruker, Billerica, MA, USA) was used to identify the composition of the synthesized nanozymes. An infrared spectrometer (Thermo Scientific Nicolet, Waltham, MA, USA) was applied to characterize the modified groups on the surface of the nanozymes. The Field Emission Transmission Electron Microscopy (FEI Company, Hillsboro, OR, USA) was utilized to analyze the morphology and elemental mapping of the nanozymes. The Field Emission Scanning Electron Microscopy (Hitachi, Tokyo, Japan) was used to observe the distribution of nanozyme particles on the NC membrane.

2.3. Preparation and Characterization of Nanozymes

CoFe_2O_4 peroxidase nanozymes with three particle sizes were synthesized by adjusting the input amount of $\text{CoCl}_2 \cdot 6\text{H}_2\text{O}$ following a modified solvothermal method. Briefly, 3.75 g maleic acid was fully dissolved in 40 mL of ethylene glycol. After stirring overnight, 1.35 g $\text{FeCl}_3 \cdot 6\text{H}_2\text{O}$, a certain amount of $\text{CoCl}_2 \cdot 6\text{H}_2\text{O}$, and 3.75 g NaAc were successively added into the mixed solution. After being stirred vigorously and ultrasonically for 1 h, the mixture was transferred into a Teflon-lined stainless-steel autoclave and reacted at 200°C for 12 h. Then, the obtained products were washed alternately by ethanol and deionized water for six times, and finally reserved in water. To synthesis different sizes of CoFe_2O_4 , the amount of added $\text{CoCl}_2 \cdot 6\text{H}_2\text{O}$ were 0.45 g, 0.6 g, and 0.9 g.

Fe_3O_4 peroxidase nanozymes with three particle sizes were synthesized by adjusting the input amount of $\text{FeCl}_3 \cdot 6\text{H}_2\text{O}$ following a modified solvothermal method. Briefly, a certain amount of $\text{FeCl}_3 \cdot 6\text{H}_2\text{O}$ was dissolved in 40 mL ethylene glycol. Next, 3.6 g NaAc was added into the mixed solution. After be stirring vigorously and ultrasonically for 0.5 h, the mixture was transferred into a Teflon-lined stainless-steel autoclave and reacted at 200°C for 12 h. Finally, the obtained products were washed alternately by ethanol and deionized water for six times, and dried under a -50°C vacuum for 12 h. To synthesis different sizes of Fe_3O_4 , the amount of added $\text{FeCl}_3 \cdot 6\text{H}_2\text{O}$ were 0.6 g, 0.8 g, and 1.8 g.

Transmission electron microscopy (TEM), scanning electron microscopy (SEM), X-ray crystal diffraction (XRD), energy-dispersive X-ray spectroscopy (EDS), X-ray photoelectron

spectroscopy (XPS), and Fourier transform infrared spectroscopy (FTIR) were used to characterize the synthesized nanozymes.

2.4. Exhibition of Migration State of Nanozymes on NC Membrane

Referring to the specific parameters of the NC membrane: the width is 2.5 cm, the chromatography speed is 134.3 s/4 cm, and the chromatography time of the NC membrane insertion hole is set to 84 s. Prepare different concentrations of nanozyme solutions with deionized water: 0.1 mg/mL, 0.2 mg/mL, 1 mg/mL; fully sonicate the above nanozyme solution and shake before use to ensure that there is no precipitation in the solution. A total of 70 μ L of nanozyme solution was pipetted, then added to the well plate and the NC membrane was immediately inserted. After 84 s, the NC membrane was taken out and completely immersed in the chromogenic solution (DAB solution or TMB solution). After 5 min, the developed NC membrane was taken out and the surface color change was recorded by taking pictures with a smart phone. The NC membrane we used was attached to a polyvinyl chloride (PVC) plate and evenly cut into 3 mm width strips. All the steps were conducted at room temperature.

2.5. Determination of Specific Activity of Nanozymes

To prepare different concentrations of nanozyme aqueous solution, the reaction system consists of 1.8 mL pH 4.5 0.2 mol/L NaAc buffer solution, 0.1 mL nanozyme solution of a certain concentration, 0.1 mL 10 mg/mL TMB solution (DMSO dissolved), and 0.2 mL 10 mol/L H_2O_2 . The above solutions were added sequentially in a quartz cuvette, and the change in absorbance of the reaction solution at 652 nm within 1 min was measured using a UV spectrophotometer, and the specific activity of the nanozyme was calculated by graphing [26]. All the measurements were conducted at 37 °C.

2.6. Determination of Zeta Potential and PDI of Nanozymes

To measure the zeta potential, 0.01 mg/mL nanozyme solution was prepared with deionized water, and 1.6 mL of the solution was pipetted into a cuvette after 5 min of ultrasonication, followed by insertion of the electrode, and the cuvette was placed in the particle size and zeta potential analyzer. Each sample was measured for 3 cycles. PDI was measured similarly, and 0.01 mg/mL nanozyme solution was prepared with deionized water. After 5–10 min of ultrasonication, 1.8 mL of the solution was immediately pipetted into a cuvette, and subsequently placed in the particle size and zeta potential analyzer. Each sample was measured for 3 cycles. All the above measurements were conducted at 25 °C.

2.7. Observation of Nanozyme Distributed on NC Membrane by SEM

A total of 70 μ L of 0.1 mg/mL nanozyme solution was added into the well plate and the NC membrane was quickly inserted. After 84 s, the NC membrane was taken out and transferred to a 37 °C oven for drying. After drying completely, SEM was used to observe the nanozyme particles at the bottom and middle of the NC membrane, and the energy dispersive spectroscopy (EDS) element scanning was used to scan the middle of the NC film for Fe and Co elements.

2.8. Preparation of 1F12-Conjugated Carboxyl-Modified Nanozymes

The nanozyme probes were synthesized by the formation of an amido bond [27,28] between the residual carboxyl group of the nanozyme and the amino group of 1F12 mAb. Briefly, 500 μ g peroxide nanozyme were first activated with 5 mM EDC and NHS solution (50 mM MES, pH 5.0). After incubation for 30 min at room temperature, the supernatant was removed by magnetic separation. The nanozyme was resuspended by adding 500 μ L 0.1 mg/mL 1F12 antibody solution, mixed thoroughly, and reacted overnight at 4 °C. The mixture was removed from the supernatant by magnetic separation and 500 μ L, 50 mM pH 7.4 Tris-HCl was immediately added. After shaking at room temperature for 30 min,

5% BSA (10 mM PBS) was added to block the non-specific binding sites on the nanozyme surface. After incubation for 60 min at room temperature, the supernatant was removed by magnetic separation and 500 μ L of PBS (10 mM pH 7.4, 0.01% Tween20) was added to resuspend the precipitate, at which time the concentration of the resulting probe was 1 mg/mL. The probe solution was stored at 4 °C for further use.

2.9. Assembly of Nanozyme-Strip

The main components of the nanozyme-strip used include NC membrane, absorbent pad and polyvinyl chloride (PVC) plate. The recombinant Anti-beta Amyloid antibody and goat anti-mouse IgG were immobilized on the NC membrane to form the detection area and quality control area, and dried at 37 °C for 2 h. Firstly, the antibody-coated NC membrane was attached to a PVC plate, and the absorbent pad was then placed on the top of the NC membrane by overlapping 2 mm. After assembly, the plate was evenly cut into 3 mm width strips, sealed with a desiccant, and stored at room temperature.

2.10. Detection of A β 42Os on Nanozyme-Strip

A range of standard solutions of A β 42Os was prepared by diluting the A β 42Os stock solution with 50 mM TBS. When testing, 70 μ L of antigen solution and 2 μ L of nanozyme probe was mixed in the sample well and the test strip was inserted. After 10 min of chromatography, the reacted test strip was taken out and immersed in a commercial DAB chromogenic solution. After immersion for 5 min, the reacted test strip was washed with water for several times, and subjected to qualitative and quantitative measurements. The photographs of the test strips were recorded by a smartphone. We converted the color of T lines into the grey value by ImageJ, then constructed the linear relation between the concentration of A β 42Os and the signal intensity.

3. Results

3.1. Characterization of Fe₃O₄ and CoFe₂O₄ Nanozymes

Fe₃O₄ nanozyme [12] and CoFe₂O₄ nanozyme [11] with different sizes were synthesized by the solvothermal method in accordance with previous reports with slight modifications, and their morphologies were observed by TEM and SEM. TEM results show that three particle sizes of Fe₃O₄ nanozymes were synthesized: 34 \pm 6 nm Fe₃O₄-1 (n = 30) (Figure 1a), 64 \pm 9 nm Fe₃O₄-2 (Figure 1b), and 184 \pm 12 nm Fe₃O₄-3 (Figure 1c); and three particle sizes of CoFe₂O₄ nanozymes: 55 \pm 6 nm CoFe₂O₄-1 (Figure 1d), 91 \pm 7 nm CoFe₂O₄-2 (Figure 1e), and 146 \pm 10 nm CoFe₂O₄-3 (Figure 1f). The morphology of Fe₃O₄-1 (Figure 1g) and Fe₃O₄-2 (Figure 1h) were irregularly spherical and heavily aggregated, and Fe₃O₄-3 (Figure 1i) was spherical; SEM show that CoFe₂O₄-1 (Figure 1j), CoFe₂O₄-2 (Figure 1k), and CoFe₂O₄-3 (Figure 1l) were spherical. The particle size distributions were shown in Figure S1.

Synthesized Fe₃O₄ nanoparticles and CoFe₂O₄ nanoparticles were both analyzed by X-ray crystal diffraction (XRD). The XRD spectra of different particle sizes of Fe₃O₄ in Figure 2a matched the Fe₃O₄ standard card exactly. Moreover, the energy-dispersive X-ray spectroscopy (EDS) mapping (Figure 2j–m) and X-ray photoelectron spectroscopy (XPS) were also measured to verify the successful synthesis of Fe₃O₄ (Figure S3), and the results indicate that the synthesized nanoparticles were all Fe₃O₄. Figure 2b shows that the XRD patterns of the synthesized CoFe₂O₄ can well match with the CoFe₂O₄ standard card, except that the characteristic peak at about 55° is not distinct. Local analysis of the XRD patterns of CoFe₂O₄ shows that there was a weak diffraction peak at approximately 55°. Compared with the diffraction peaks of Fe₃O₄, the diffraction peaks of CoFe₂O₄ are significantly broadened, attributing to the difference in the ionic radius of Co and Fe ions. Moreover, the diffraction peak at about 43° is not shown in the XRD patterns of CoFe₂O₄ due to the broadening effect of the diffraction peak at 41°. These results indicates that Co is involved in the synthesis of CoFe₂O₄. The energy-dispersive X-ray spectroscopy (EDS) mapping (Figure 2e–j) demonstrates the presence of Co in CoFe₂O₄ nanozyme, and X-ray

photoelectron spectroscopy (XPS) was further used to prove the successful synthesis of CoFe_2O_4 (Figure S2).

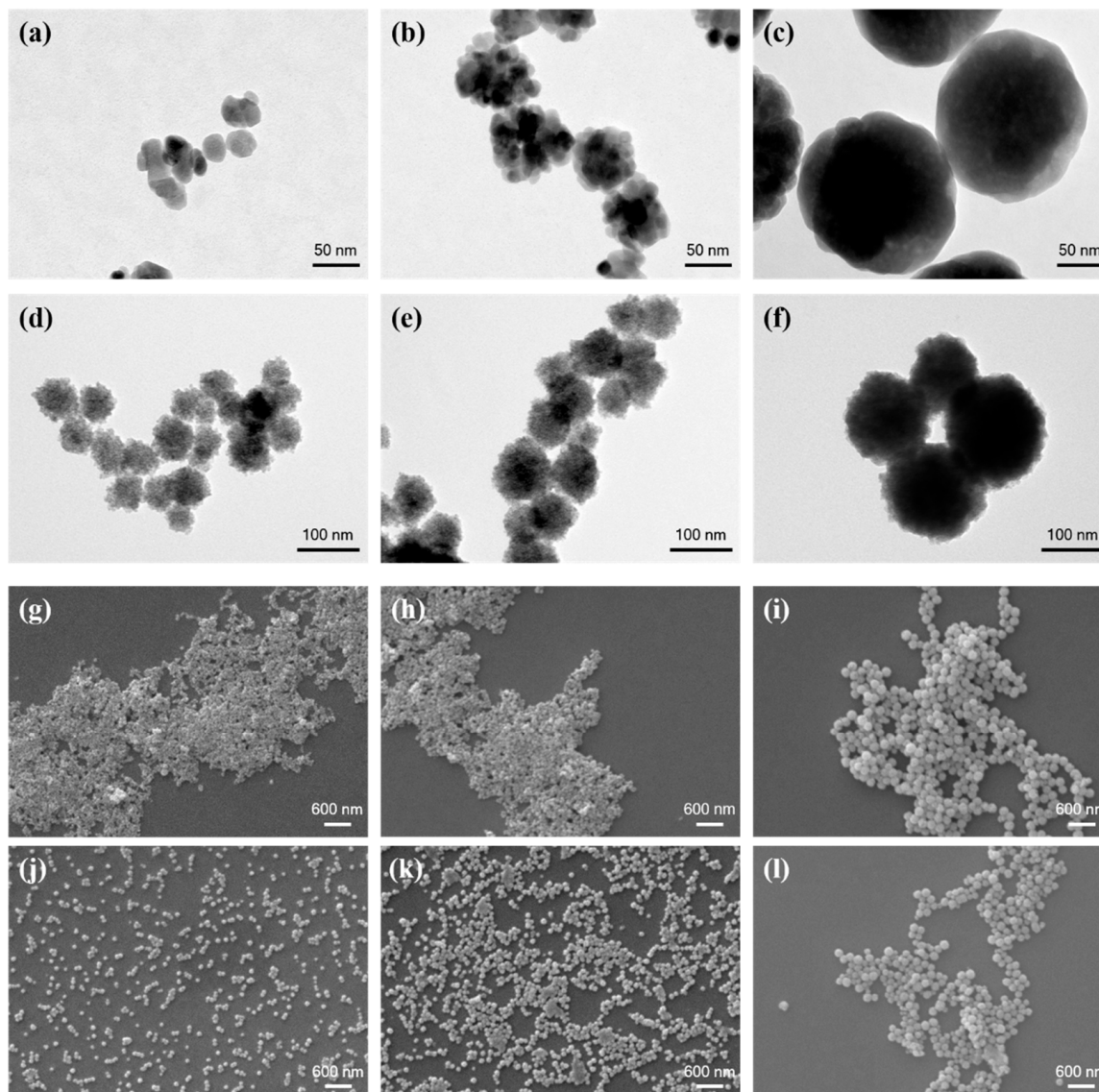


Figure 1. Characterization of CoFe_2O_4 nanozyme and Fe_3O_4 nanozyme by TEM and SEM. (a–c) TEM images of Fe_3O_4 nanozymes with different sizes. (d–f) TEM images of CoFe_2O_4 nanozymes with different sizes. (g–i) SEM images of Fe_3O_4 nanozymes with different sizes. (j–l) SEM images of CoFe_2O_4 nanozymes with different sizes.

NaAc was added during the synthesis process in order to make the nanoparticles with carboxyl groups, Fourier transform infrared spectrum (FTIR) was utilized to analyze the modified groups on the surface of CoFe_2O_4 and Fe_3O_4 nanozymes. In Figure 2c, the vibrational peaks near 1560 cm^{-1} and 3410 cm^{-1} for CoFe_2O_4 nanozyme correspond to $\text{C}=\text{O}$ and $-\text{OH}$ vibrations, respectively, indicating the presence of carboxyl groups on the surface of CoFe_2O_4 nanoparticles; Figure 2d shows that the vibrational peaks of Fe_3O_4 nanozyme near 1630 cm^{-1} and 3400 cm^{-1} correspond to $\text{C}=\text{O}$ and $-\text{OH}$ vibrations, respectively, indicating the presence of carboxyl group modification on the surface of Fe_3O_4 nanoparticles as well [29,30].

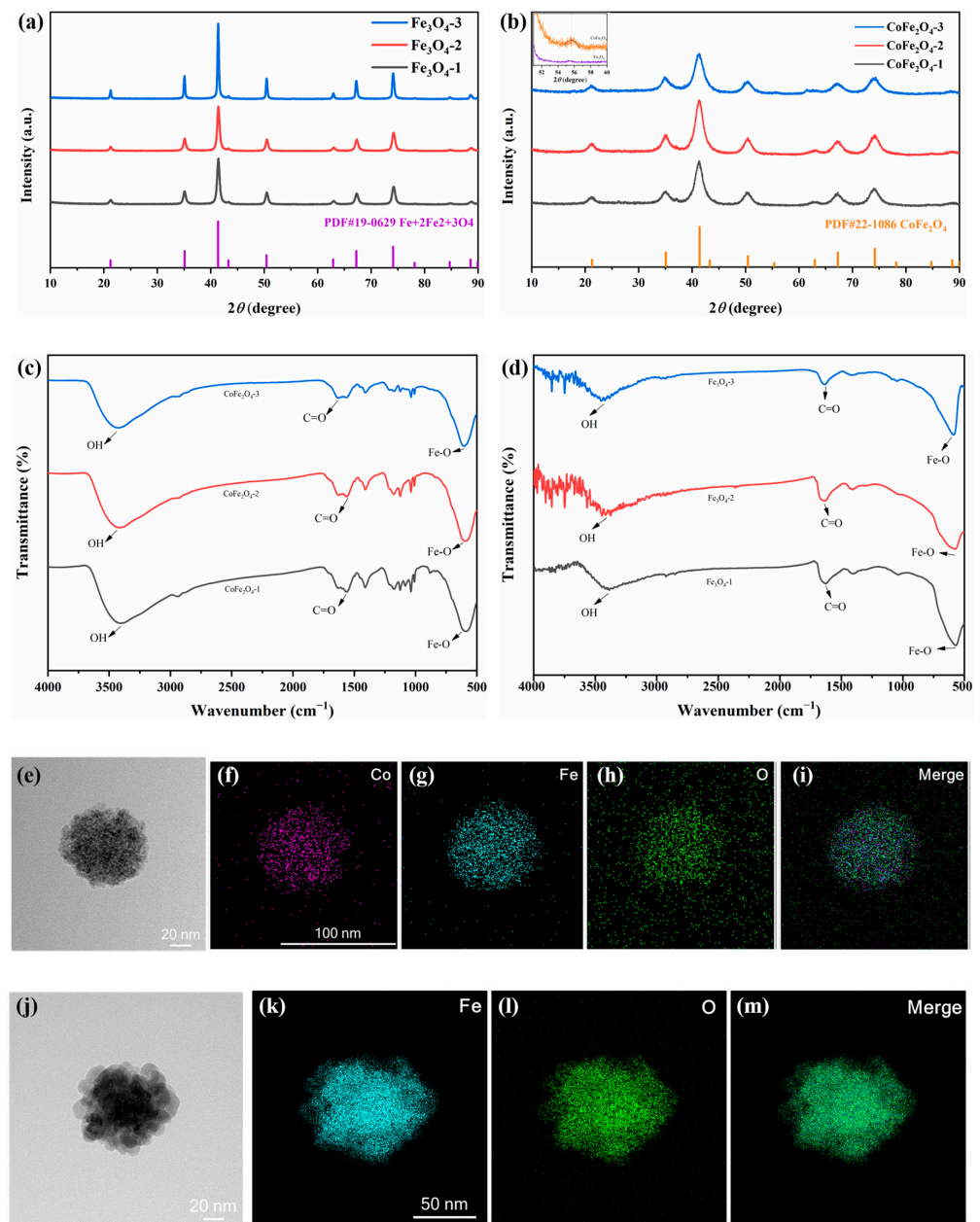


Figure 2. Characterization of CoFe_2O_4 nanozyme and Fe_3O_4 nanozyme by XRD and FTIR. (a) XRD spectrum of Fe_3O_4 nanozymes. (b) XRD spectrum of CoFe_2O_4 nanozymes. (c) FTIR of CoFe_2O_4 nanozymes. (d) FTIR of Fe_3O_4 nanozymes. (e–i) Images of TEM and corresponding EDS elemental mapping of CoFe_2O_4 nanozyme. (j–m) Images of TEM and corresponding EDS elemental mapping of Fe_3O_4 nanozyme.

3.2. Characterization of Nanozymes on NC Membrane by Color Development

The NC membranes distributed with CoFe_2O_4 nanozymes were developed in DAB and TMB solution, and had significant color change on their surface. With increasing nanoparticle concentration: 0.1 mg/mL, 0.2 mg/mL, and 1 mg/mL (Figure 3b,c), the color of NC membranes had a tendency to deepen. In Fe_3O_4 group, a large number of nanoparticles can be observed on the bottom part of the NC membranes before color development, and there was almost no color change on its surface after color development (Figure 3b,c) compared with control NC membrane, indicating that CoFe_2O_4 nanozymes performed better on NC membrane. When the concentration of CoFe_2O_4 solution increased to 1 mg/mL, the color of the nanoparticles largely overwhelmed the color of the blue

oxidation products of TMB, the phenomenon might affect the signal amplification of detection on nanozyme-strip. Moreover, the color development effect of DAB on the NC membrane became more and more distinct with the increasing concentration of the nanozyme solution, indicating that a better effect on NC membrane was achieved by using DAB. Hence, we chose DAB as the chromogenic solution in the later nanozyme-strip assay.

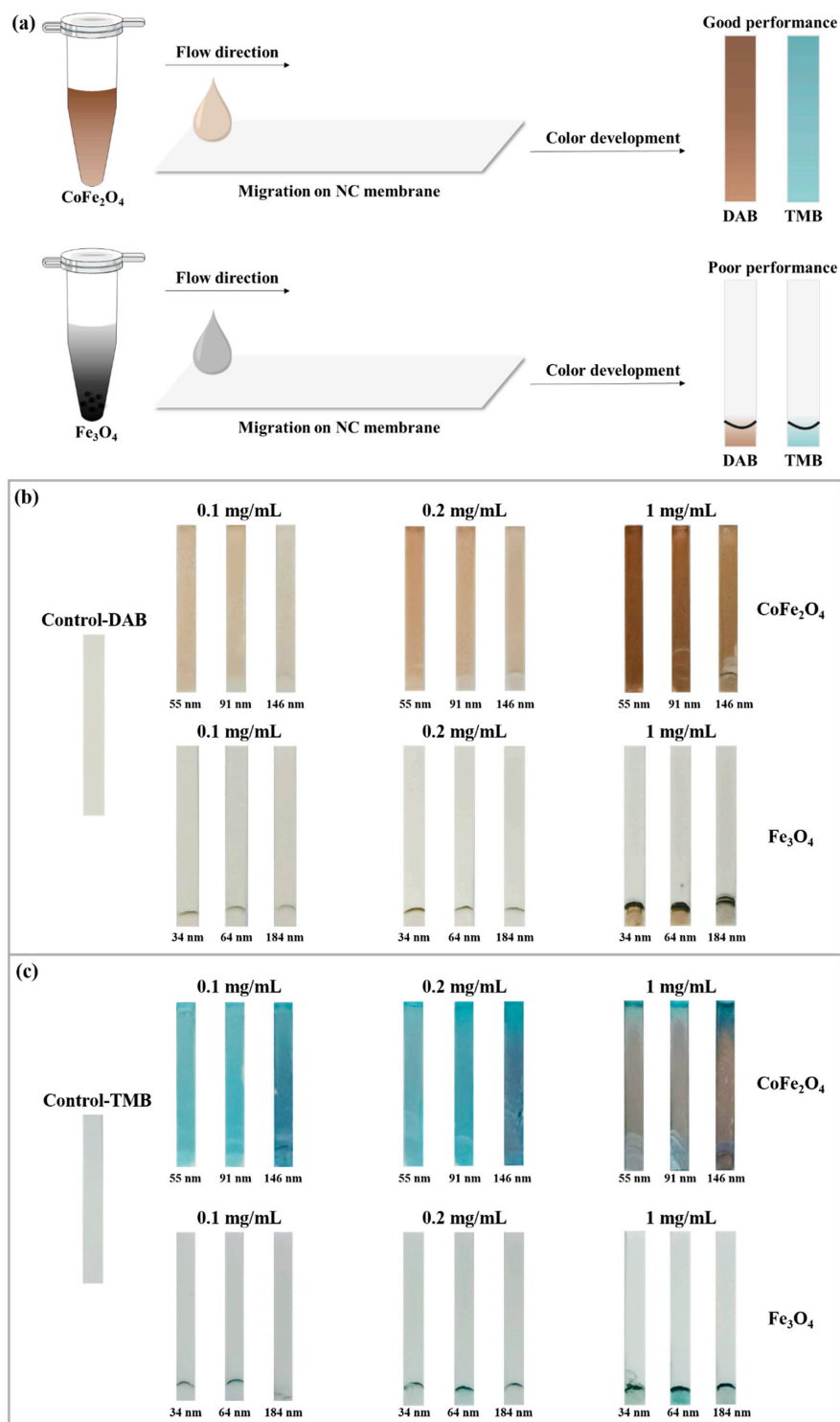


Figure 3. In situ color development of nanozymes on NC membrane. (a) A comprehensive scheme of the experimental process and result evaluation. (b) Exhibition of nanozymes on NC membrane by DAB substrate solution. (c) Exhibition of nanozymes on NC membrane by TMB substrate solution.

The POD activities of the two nanozymes were compared, and Figure 4a shows that the OD652 nm values of TMB reaction catalyzed by different particle sizes of CoFe_2O_4 peroxide nanozymes were in the range of 2.53–2.60 at 285 s, while the OD652 nm values of different particle sizes of Fe_3O_4 peroxide nanozymes were in the range of 0.16–0.25. Further, their POD-specific activities were determined [26], the POD-specific activity of CoFe_2O_4 -1, CoFe_2O_4 -2, and CoFe_2O_4 -3 were 5.929 U/mg, 5.511 U/mg, and 5.165 U/mg, respectively; and the POD-specific activity of Fe_3O_4 -1, Fe_3O_4 -2, and Fe_3O_4 -3 were 0.404 U/mg, 0.483 U/mg, and 0.292 U/mg, respectively. The results show that the POD-specific activity of CoFe_2O_4 was significantly higher than that of Fe_3O_4 (Figure 4b).

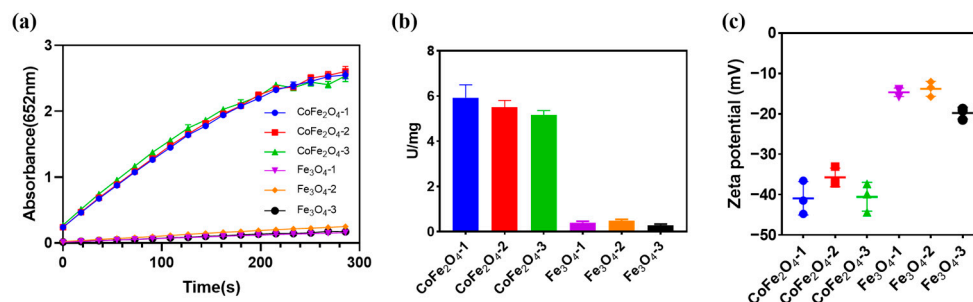


Figure 4. Comparison of peroxidase-like activity and surface charge between CoFe_2O_4 nanozymes and Fe_3O_4 nanozymes. (a) Time curve of TMB reaction catalyzed by nanozymes. (b) Comparison of POD-specific activity among CoFe_2O_4 nanozymes and Fe_3O_4 nanozymes. (c) Zeta potential measurements indicating good dispersity of CoFe_2O_4 nanozymes.

Zeta potential is an important indicator to characterize the stability of a dispersion system. We measured the zeta potentials of CoFe_2O_4 and Fe_3O_4 nanozymes separately. The zeta potentials of CoFe_2O_4 -1, CoFe_2O_4 -2, and CoFe_2O_4 -3 were -40.93 mV, -35.75 mV, and -40.55 mV, respectively; the zeta potentials of Fe_3O_4 -1, Fe_3O_4 -2, and Fe_3O_4 -3 were -14.68 mV, -13.79 mV, and -19.82 mV, respectively. Figure 2e revealed that the absolute values of zeta potential of CoFe_2O_4 group were significantly higher than those of Fe_3O_4 group. These results indicate that CoFe_2O_4 nanozymes had better dispersion than Fe_3O_4 nanozymes. Meanwhile, their polymer dispersion index (PDI) was measured, and the PDI of CoFe_2O_4 nanoparticles is in the range of 0.05~0.06, while that of Fe_3O_4 nanoparticles is in the range of 0.25~0.27 (Table S1).

3.3. Characterization of CoFe_2O_4 Nanozymes on NC Membrane by SEM

The surface of the undeveloped NC membranes distributed with CoFe_2O_4 nanoparticles were observed by SEM, and each of its bottom and middle parts were observed. Compared with the blank NC membrane (Figure 5a,b), Figure 5h shows that the bottom of CoFe_2O_4 -3-NC membrane has a large number of nanoparticles (pointed out by the red arrow) distributed, while the middle part (Figure 5g) has very few nanoparticles distributed compared with the CoFe_2O_4 -3-NC membrane. Both CoFe_2O_4 -1-NC membrane and CoFe_2O_4 -2-NC membrane have fewer nanoparticles at the bottom (Figure 5d,f), but more nanoparticles at the middle part of membranes (Figure 5c,e). The surface of the undeveloped NC membranes distributed with Fe_3O_4 nanoparticles were also observed by SEM. Compared with the blank NC membrane, numerous Fe_3O_4 nanoparticles were aggregated at the bottom part of the NC membranes (Figure S4b,d,f,h), and at the middle part of the NC membranes it was hard to find nanoparticles (Figure S4a,c,e,g). The results indicate that the NC membrane had color change in the distance from the bottom to the black belt when the concentration of Fe_3O_4 solution was 1 mg/mL. These results indicate that Fe_3O_4 nanoparticles failed to migration forward after the aggregation occurred on the NC membrane.

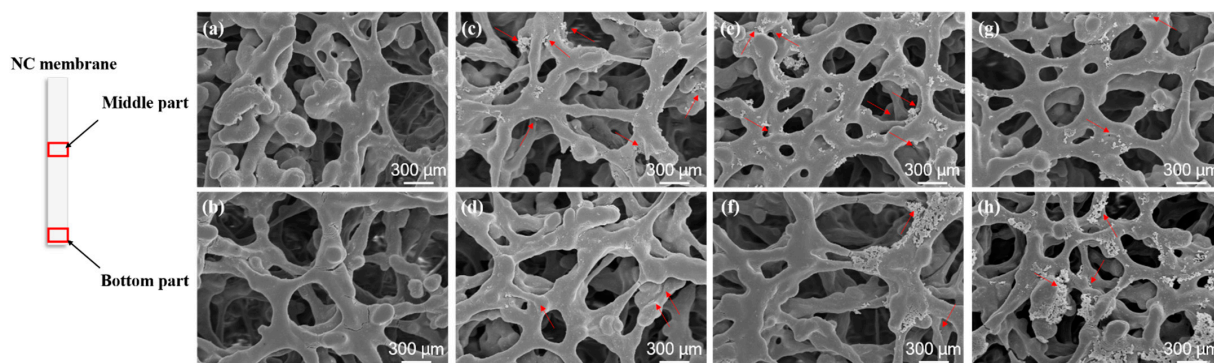


Figure 5. Characterization of CoFe_2O_4 nanozymes on NC membrane by SEM. (a) Middle part of blank NC membrane. (b) Bottom part of blank NC membrane. (c) Middle part of CoFe_2O_4 -1-NC membrane. (d) Bottom part of CoFe_2O_4 -1-NC membrane. (e) Middle part of CoFe_2O_4 -2-NC membrane. (f) Bottom part of CoFe_2O_4 -2-NC membrane. (g) Middle part of CoFe_2O_4 -3-NC membrane. (h) Bottom part of CoFe_2O_4 -3-NC membrane. Red arrows are used to point out the nanozymes.

EDS elemental surface scan was performed on the middle part of the undeveloped NC membranes for Fe and Co elements (Figure 6a), and the average signal intensity of each Merge image was analyzed using ImageJ. Figure 6b shows that the average signal intensities of the nanozymes distributed on the surface of CoFe_2O_4 -1-NC, CoFe_2O_4 -2-NC, and CoFe_2O_4 -3-NC membranes were 50.413, 50.267, and 34.104, respectively. The average signal intensities of Fe and Co elements in the middle of the CoFe_2O_4 -3-NC membrane were significantly lower than those of CoFe_2O_4 -1-NC and CoFe_2O_4 -2-NC membranes, suggesting that the size of nanoparticles may affect their migration on the NC membrane. This result was consistent with the SEM observation. Combined with the results of nanoparticle distribution on NC membrane characterized by DAB solution (Figure 3b), CoFe_2O_4 -1 has better color development effect than CoFe_2O_4 -2 on NC membrane and was eventually chosen for the preparation of nanozyme probes.

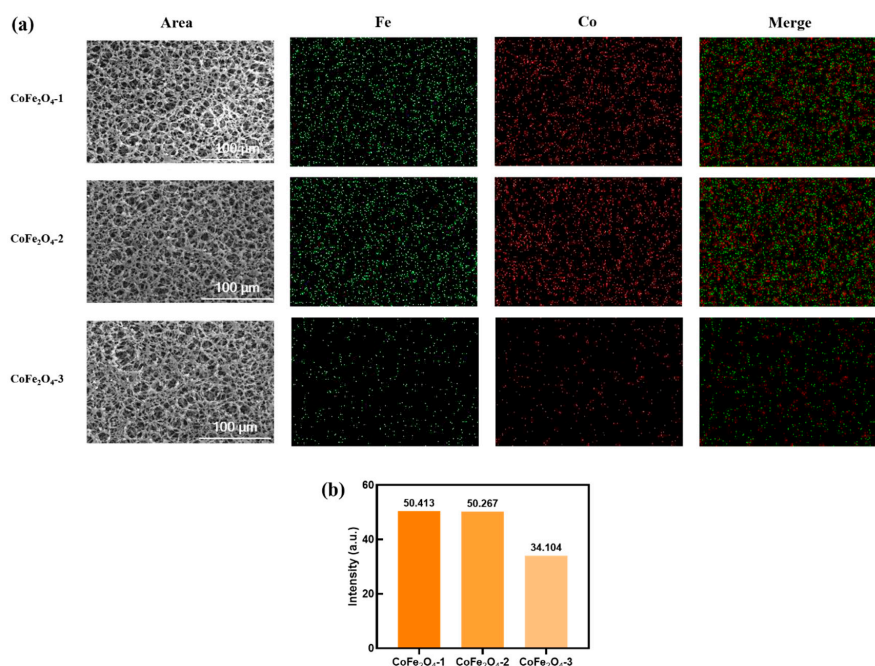


Figure 6. Distribution of nanozymes on NC membrane characterized by EDS. (a) EDS surface scanning of NC membrane distributing CoFe_2O_4 nanozymes. (b) Mean signal strength of three merge images.

3.4. Detection of A β 42Os with Nanozyme Test Probe

The nanozyme probe for detecting A β 42 oligomers (A β 42Os) was prepared by using the CoFe₂O₄-1 nanozyme that performed best on the NC membrane, and its performance on the nanozyme-strip was tested. A β 42Os is a biomarker of AD, and A β 42Os in blood has the potential to diagnose AD. The oligomer form in the A β 42Os stock solution used in the experiment is mainly a trimer. Figure 7a depicts the principle of CoFe₂O₄-1 nanozyme probe for highly sensitive detection of A β 42Os. Figure 7b shows that the nanozyme probe can detect A β 42Os in the concentration range of 0.18–1820 ng/mL, and there was no retention of the nanozyme probe at the bottom of the NC membrane. In order to evaluate the performance of A β 42Os testing by nanozyme-strip, the signal intensity of T line was analyzed by ImageJ. There was a good correlation ($R^2 = 0.9796$) between the T line signal intensity and the detection concentration within the concentration range of 0.18–1820 ng/mL (Figure 7c). Previous studies have reported that the A β 42Os levels in the blood of AD patients range from 0.1 to 1 ng/mL, as detected by sandwich ELISA [31]. The sensitivity of the nanozyme-strip for A β 42Os detection needs to be improved.

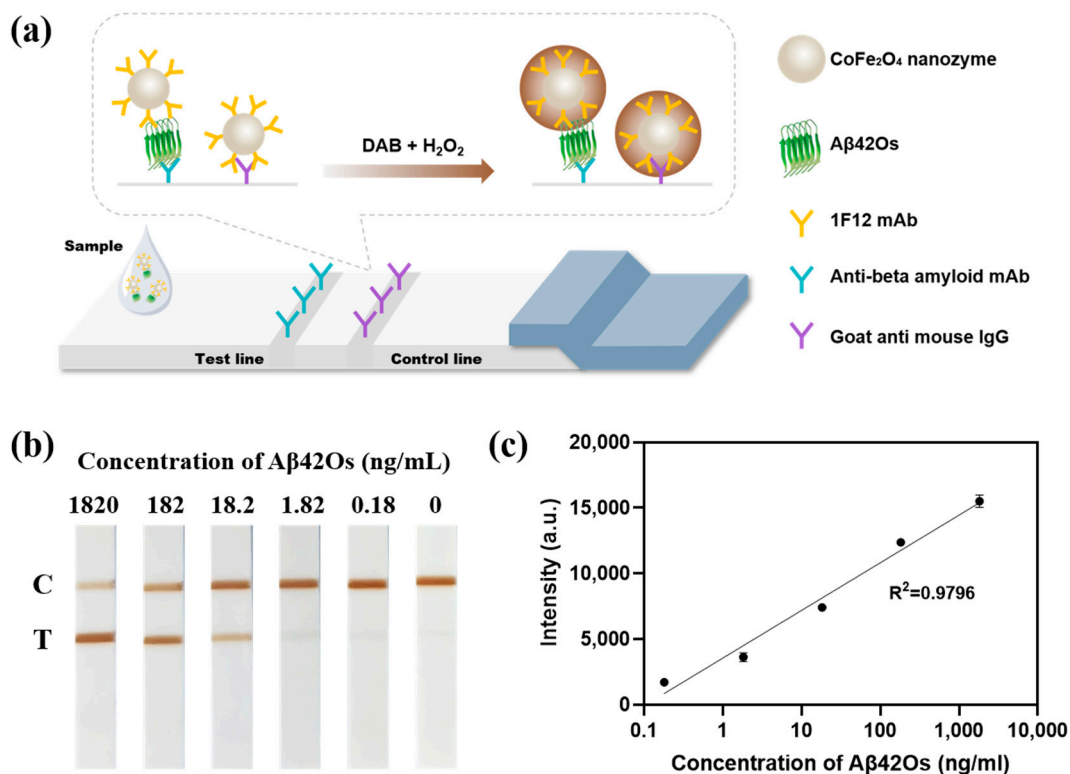


Figure 7. A β 42Os detection by nanozyme-strip based on CoFe₂O₄-1 nanozyme probe. (a) Illustration of nanozyme-strip for A β 42Os detection. (b) Detection of A β 42Os with CoFe₂O₄-1 nanozyme-strip. (c) Relative analysis of signal intensity regarding T lines.

4. Discussion

The nanozyme applied to the nanozyme-strip needs to migrate smoothly on the NC membrane without aggregation during the lateral movement, so that more nanozyme probes can reach the detection area and achieve the high-sensitivity detection of target [32].

To investigate the migration of CoFe₂O₄ and Fe₃O₄ nanozymes on NC membrane, the NC membranes distributed with the nanozymes were developed by peroxidase substrate solution (DAB or TMB). The nanozymes with POD-like enzyme activity can catalyze the peroxidase substrates to colored products which deposit on the surface of the NC membranes, leading to a significant color change (the oxidation of DAB produces a brown color product; the oxidation of TMB produces a blue color product). The color of NC

membranes in CoFe₂O₄ group was much deeper than that in Fe₃O₄ group, and the NC membrane distributed with CoFe₂O₄-1 nanozymes had the darkest color under the same concentration (Figure 3b). The POD activity of CoFe₂O₄ nanozymes with different particle sizes had no significant difference (Figure 4c). A possible explanation might be that the largest number and even distribution of CoFe₂O₄-1 nanoparticles per unit area makes the NC membrane the deepest after color development. In previous studies of the nanozyme-strip, researchers mainly focused on the activity of nanozymes. Our study shows that enzyme-like activity should not be the only factor to be considered but also the dispersibility of the nanozyme should be taken into account. Zeta potential is an important parameter to reflect the charged state of the particle surface in the suspension, which can be used to analyze the stability of nanoparticles in the dispersion system [33]. The absolute value of the Zeta potential of CoFe₂O₄ nanoparticles with three particle sizes was significantly higher than that of Fe₃O₄ nanoparticles with three particle sizes. However, there is no significant difference in the absolute value of Zeta potential within the group. Owing to the low absolute value of the zeta potential, the attraction between Fe₃O₄ particles is greater than the repulsive force, resulting in the aggregation of nanoparticles and failing to move on the NC membrane after migrating a short distance.

In order to compare the distribution of CoFe₂O₄ nanozymes with three particle sizes on the NC membrane, the surface of the NC membranes was observed by SEM. SEM shows that there were a large number of nanoparticles distributed at the bottom of the CoFe₂O₄-3-NC membrane and very few in the middle zone, which demonstrated that the CoFe₂O₄-3 distribution on the CoFe₂O₄-3-NC membrane was uneven and mostly distributed at the bottom. Further, EDS was used to scan the middle part of these NC membranes for Fe and Co elements, the signal intensity of Fe and Co elements on CoFe₂O₄-3-NC membrane was significantly lower than that of CoFe₂O₄-1-NC membrane and CoFe₂O₄-2-NC membrane, indicating that a fewer number of CoFe₂O₄-3 nanoparticles moved to the middle of the NC membrane. We speculated that the migration of nanozymes with good dispersity would be also affected when the nanoparticle size reaches a certain level. The distribution of CoFe₂O₄-1 and CoFe₂O₄-2 on NC membrane did not show significant differences, but the NC membrane distributed with CoFe₂O₄-1 had the darkest color. We selected CoFe₂O₄-1 nanozyme, which performed the best on the NC membrane from the candidates to prepare the nanozyme probe for detecting Aβ₄₂Os by a comprehensive evaluation of three aspects: dispersibility, distribution on the NC membrane, and the level of POD activity. In the presence of Aβ₄₂Os, the CoFe₂O₄-1 nanozyme probe did not show aggregation and retention on the NC membrane, T lines and C lines appeared on its surface after color development. The experimental results showed that the probe can migrate forward smoothly on the NC membrane (Figure 7b), and the detection of Aβ₄₂Os was realized. At the same time, for the detection of Aβ₄₂Os, more optimization studies are needed to improve the sensitivity of the nanozyme-strip. In summary, the selected CoFe₂O₄-1 nanozyme can be applied to the nanozyme-strip, and has the potential to be widely used to prepare nanozyme probes for different targets.

The Fe₃O₄ nanozyme with poor dispersion only migrated a short distance on the NC membrane before aggregation occurred, and failed to move to the detection area on the NC membrane; whereas CoFe₂O₄ nanozymes had better dispersion and could migrate forward on the NC membrane, and a large amount of CoFe₂O₄ nanozymes could reach the detection area of the NC membrane. Although the particle size of Fe₃O₄-1 nanoparticles is smaller than that of CoFe₂O₄-1 nanoparticles, poor dispersion of Fe₃O₄-1 nanoparticles led to its aggregation during migration on the NC membrane, and it could not migrate forward as smoothly as CoFe₂O₄-1 nanoparticles, resulting in a vast number of nanoparticles accumulated at the bottom of the NC membrane. Hence, we considered that dispersity is the most important parameter for nanozyme applied to nanozyme-strip. Dispersity affects the movement of nanozymes on the NC membrane. The nanozyme probe prepared by nanozymes with better dispersion migrate more to the detection zone, which is beneficial for the results. For nanozymes with good dispersion, we can optimize them in

terms of particle size and enzyme-like activity to further improve the performance of the nanozyme-strip.

Meanwhile, both CoFe_2O_4 nanozyme and Fe_3O_4 nanozyme have been reported to show superparamagnetic properties [11,12]. Nanozymes with magnetic response can be used to enrich the analytes in the sample to improve the detection sensitivity of the nanozyme-strip, and the magnetic separation of nanozymes can also simplify the preparation of nanozyme probes. Nanozymes with magnetic properties and good dispersity are ideal for nanozyme probes. The study of nanozyme-strips should focus on the synthesis of nanozymes with such properties.

5. Conclusions

We optimized the nanozyme-strip by using candidate nanozymes synthesized in the laboratory, focusing on the nanozyme migration state on the NC membrane. The migration state of the nanozyme probe on the NC membrane greatly affects the detection ability of the nanozyme-strip. Dispersity of the nanozyme dominates its migration state on the NC membrane. Zeta potential and PDI value of nanozymes can indirectly forecast its movement on the NC membrane: the higher the absolute value of the zeta potential (>35 mV), the smaller the PDI value (0.05 level), and the better dispersion of the nanozyme, the less likely it is to aggregate on the NC membrane. More attention should be paid to the dispersion of nanozymes when screening nanozymes to prepare the detection probe for the nanozyme-strip. The migration and distribution of nanozymes on the NC membrane and the enzyme-like activity should be comprehensively investigated, and the best-performed nanozyme is screened out among the candidate nanozymes for the preparation of detection probes so as to achieve high-sensitivity detection of the target, which can also save the use of antibodies and reduce the development cost of nanozymes-strips. The work of this paper aims to promote the research of nanozyme-strips.

Supplementary Materials: The following supporting information can be downloaded at: <https://www.mdpi.com/article/10.3390/s23073414/s1>. Figure S1: Particle size distribution of nanozymes (a) Fe_3O_4 -1 nanozyme, (b) Fe_3O_4 -2 nanozyme, (c) Fe_3O_4 -3 nanozyme, (d) CoFe_2O_4 -1 nanozyme, (e) CoFe_2O_4 -2 nanozyme, (f) CoFe_2O_4 -3 nanozyme. Figure S2: Characterization of CoFe_2O_4 nanozyme by XPS. (a) Survey spectra of CoFe_2O_4 . (b) High-resolution spectra of Fe 2p. (c) High-resolution spectra of Co 2p. (d) High-resolution spectra of O 1s. Figure S3: Characterization of Fe_3O_4 nanozyme by XPS. (a) Survey spectra of Fe_3O_4 . (b) High-resolution spectra of Fe 2p. (c) High-resolution spectra of O 1s. Figure S4: Characterization of Fe_3O_4 nanozymes on NC membrane by SEM. (a) Middle part of blank NC membrane. (b) Bottom part of blank NC membrane. (c) Middle part of Fe_3O_4 -1-NC membrane. (d) Bottom part of Fe_3O_4 -1-NC membrane. (e) Middle part of Fe_3O_4 -2-NC membrane. (f) Bottom part of Fe_3O_4 -2-NC membrane. (g) Middle part of Fe_3O_4 -3-NC membrane. (h) Bottom part of Fe_3O_4 -3-NC membrane. Table S1: PDI of nanozymes detected by DLS.

Author Contributions: Conceptualization, L.G.; methodology, Y.L. and L.G.; validation, Y.L. and L.G.; investigation, Y.L.; data curation, Y.L.; resources, Y.L., H.L. and S.Z.; writing-original draft preparation, Y.L. and D.D.; writing-review and editing L.G., L.C., J.J. and Y.L.; supervision, Y.L. and L.G. All authors have read and agreed to the published version of the manuscript.

Funding: This study was supported by National Key R&D Program of China (2019YFA0709200), National Natural Science Foundation of China Foundation of Innovative Research Group grant (22121003).

Institutional Review Board Statement: Not applicable.

Informed Consent Statement: Not applicable.

Data Availability Statement: The data presented in this study are available on request from the corresponding author.

Acknowledgments: We thank the Testing and Analysis Centre and the Center for Biological Imaging (CBI) at the Institute of Biophysics, Chinese Academy of Sciences (CAS), for characterization of nanomaterials. We thank Liding Zhang from MoE Key Laboratory for Biomedical Photonics, School

of Engineering Sciences, Huazhong University of Science and Technology for supplying us 1F12 monoclonal antibody.

Conflicts of Interest: The authors declare no conflict of interest.

References

1. Frew, E.; Roberts, D.; Barry, S.; Holden, M.; Restell Mand, A.; Mitsok, E.; Tan, E.; Yu, W.; Skog, J. A SARS-CoV-2 antigen rapid diagnostic test for resource limited settings. *Sci. Rep.* **2021**, *11*, 23009. [[CrossRef](#)] [[PubMed](#)]
2. Wang, Y.; Deng, R.G.; Zhang, G.P.; Li, Q.M.; Yang, J.F.; Sun, Y.N.; Li, Z.X.; Hu, X.F. Rapid and Sensitive Detection of the Food Allergen Glycinin in Powdered Milk Using a Lateral Flow Colloidal Gold Immunoassay Strip Test. *J. Agric. Food Chem.* **2015**, *63*, 2172–2178. [[CrossRef](#)] [[PubMed](#)]
3. Xu, Q.F.; Xu, H.; Gu, H.C.; Li, J.B.; Wang, Y.Y.; Wei, M. Development of lateral flow immunoassay system based on superparamagnetic nanobeads as labels for rapid quantitative detection of cardiac troponin I. *Mater. Sci. Eng. C* **2009**, *29*, 702–707. [[CrossRef](#)]
4. Hong, L.X.; Wang, K.; Yan, W.Q.; Xu, H.; Chen, Q.H.; Zhang, Y.H.; Cui, D.X.; Jin, Q.H.; He, J.H. High performance immunochromatographic assay for simultaneous quantitative detection of multiplex cardiac markers based on magnetic nanobeads. *Theranostics* **2018**, *8*, 6121–6131. [[CrossRef](#)] [[PubMed](#)]
5. Chang, R.; Cai, Y.; Wang, Z.; Peng, C. Rapid Detection of Kanamycin Based on Aptamer Colloid Gold Lateral Flow Test Strip. *J. Instrum. Anal.* **2021**, *40*, 1728–1735.
6. Bruno, J.G. Application of DNA Aptamers and Quantum Dots to Lateral Flow Test Strips for Detection of Foodborne Pathogens with Improved Sensitivity versus Colloidal Gold. *Pathogens* **2014**, *3*, 341–355. [[CrossRef](#)]
7. Mahmoudi, T.; de la Guardia, M.; Shirdel, B.; Mokhtarzadeh, A.; Baradaran, B. Recent advancements in structural improvements of lateral flow assays towards point-of-care testing. *Trac-Trends Anal. Chem.* **2019**, *116*, 13–30. [[CrossRef](#)]
8. Napione, L. Integrated Nanomaterials and Nanotechnologies in Lateral Flow Tests for Personalized Medicine Applications. *Nanomaterials* **2021**, *11*, 2362. [[CrossRef](#)]
9. Ge, X.; Liu, Z.; Zhang, W.; Guo, S. Single-Atom Nanocatalysts for Biosensing Application. *Curr. Anal. Chem.* **2022**, *18*, 753–763. [[CrossRef](#)]
10. Songca, S.P. Applications of Nanozymology in the Detection and Identification of Viral, Bacterial and Fungal Pathogens. *Int. J. Mol. Sci.* **2022**, *23*, 4638. [[CrossRef](#)]
11. Liu, D.; Ju, C.H.; Han, C.; Shi, R.; Chen, X.H.; Duan, D.M.; Yan, J.H.; Yan, X.Y. Nanozyme chemiluminescence paper test for rapid and sensitive detection of SARS-CoV-2 antigen. *Biosens. Bioelectron.* **2021**, *173*, 112817. [[CrossRef](#)] [[PubMed](#)]
12. Gao, L.; Zhuang, J.; Nie, L.; Zhang, J.; Zhang, Y.; Gu, N.; Wang, T.; Feng, J.; Yang, D.; Perrett, S.; et al. Intrinsic peroxidase-like activity of ferromagnetic nanoparticles. *Nat. Nanotechnol.* **2007**, *2*, 577–583. [[CrossRef](#)] [[PubMed](#)]
13. Wei, H.; Wang, E. Nanomaterials with enzyme-like characteristics (nanozymes): Next-generation artificial enzymes. *Chem. Soc. Rev.* **2013**, *42*, 6060–6093. [[CrossRef](#)] [[PubMed](#)]
14. Gao, L.; Chen, L.; Zhang, R.; Yan, X. Nanozymes: Next-generation artificial enzymes. *Sci. Sin. Chim.* **2022**, *52*, 1649–1663. [[CrossRef](#)]
15. Wu, J.; Wang, X.; Wang, Q.; Lou, Z.; Li, S.; Zhu, Y.; Qin, L.; Wei, H. Nanomaterials with enzyme-like characteristics (nanozymes): Next-generation artificial enzymes (II). *Chem. Soc. Rev.* **2019**, *48*, 1004–1076. [[CrossRef](#)]
16. Duan, D.; Fan, K.; Zhang, D.; Tan, S.; Liang, M.; Liu, Y.; Zhang, J.; Zhang, P.; Liu, W.; Qiu, X.; et al. Nanozyme-strip for rapid local diagnosis of Ebola. *Biosens. Bioelectron.* **2015**, *74*, 134–141. [[CrossRef](#)]
17. Chen, R.; Chen, X.; Zhou, Y.; Lin, T.; Leng, Y.; Huang, X.; Xiong, Y. “Three-in-One” Multifunctional Nanohybrids with Colorimetric Magnetic Catalytic Activities to Enhance Immunochromatographic Diagnosis. *ACS Nano* **2022**, *16*, 3351–3361. [[CrossRef](#)]
18. Meng, X.; Zou, S.; Li, D.; He, J.; Fang, L.; Wang, H.; Yan, X.; Duan, D.; Gao, L. Nanozyme-strip for rapid and ultrasensitive nucleic acid detection of SARS-CoV-2. *Biosens. Bioelectron.* **2022**, *217*, 114739. [[CrossRef](#)]
19. Fagan, A.M.; Mintun, M.A.; Mach, R.H.; Lee, S.-Y.; Dence, C.S.; Shah, A.R.; LaRossa, G.N.; Spinner, M.L.; Klunk, W.E.; Mathis, C.A.; et al. Inverse relation between in vivo amyloid imaging load and cerebrospinal fluid A β 42 in humans. *Ann. Neurol.* **2006**, *59*, 512–519. [[CrossRef](#)]
20. Haass, C.; Selkoe, D.J. Soluble protein oligomers in neurodegeneration: Lessons from the Alzheimer’s amyloid β -peptide. *Nat. Rev. Mol. Cell Biol.* **2007**, *8*, 101–112. [[CrossRef](#)]
21. Pontecorvo, M.J.; Mintun, M.A. PET amyloid imaging as a tool for early diagnosis and identifying patients at risk for progression to Alzheimer’s disease. *Alzheimer’s Res. Ther.* **2011**, *3*, 11. [[CrossRef](#)] [[PubMed](#)]
22. Shaw, L.M.; Vanderstichele, H.; Knapik-Czajka, M.; Clark, C.M.; Aisen, P.S.; Petersen, R.C.; Blennow, K.; Soares, H.; Simon, A.; Lewczuk, P.; et al. Cerebrospinal Fluid Biomarker Signature in Alzheimer’s Disease Neuroimaging Initiative Subjects. *Ann. Neurol.* **2009**, *65*, 403–413. [[CrossRef](#)] [[PubMed](#)]
23. Zhang, L.; Yang, C.; Li, Y.; Niu, S.; Liang, X.; Zhang, Z.; Luo, Q.; Luo, H. Dynamic Changes in the Levels of Amyloid-beta42 Species in the Brain and Periphery of APP/PS1 Mice and Their Significance for Alzheimer’s Disease. *Front. Mol. Neurosci.* **2021**, *14*, 723317. [[CrossRef](#)]

24. Van-Thuan, N.; Song, S.; Park, S.; Joo, C. Recent advances in high-sensitivity detection methods for paper-based lateral-flow assay. *Biosens. Bioelectron.* **2020**, *152*, 112015.
25. Jia, L.; Qiu, Q.; Zhang, H.; Chu, L.; Du, Y.; Zhang, J.; Zhou, C.; Liang, F.; Shi, S.; Wang, S.; et al. Concordance between the assessment of Aβ₄₂, T-tau, and P-T181-tau in peripheral blood neuronal-derived exosomes and cerebrospinal fluid. *Alzheimers Dement.* **2019**, *15*, 1071–1080. [[CrossRef](#)]
26. Jiang, B.; Duan, D.; Gao, L.; Zhou, M.; Fan, K.; Tang, Y.; Xi, J.; Bi, Y.; Tong, Z.; Gao, G.; et al. Standardized assays for determining the catalytic activity and kinetics of peroxidase-like nanozymes. *Nat. Protoc.* **2018**, *13*, 1506–1520. [[CrossRef](#)]
27. Tao, X.; Wang, X.; Liu, B.; Liu, J. Conjugation of antibodies and aptamers on nanozymes for developing biosensors. *Biosens. Bioelectron.* **2020**, *168*, 112537. [[CrossRef](#)]
28. Huang, X.; Zhuang, J.; Chen, D.; Liu, H.; Tang, F.; Yan, X.; Meng, X.; Zhang, L.; Ren, J. General strategy for designing functionalized magnetic microspheres for different bioapplications. *Langmuir* **2009**, *25*, 11657–11663. [[CrossRef](#)]
29. Wang, J.; Zhao, G.; Yu, F. Facile preparation of Fe₃O₄@MOF core-shell microspheres for lipase immobilization. *J. Taiwan Inst. Chem. Eng.* **2016**, *69*, 139–145. [[CrossRef](#)]
30. Li, M.; Li, Y.; Li, Z.Y.; Hu, R.; Yang, Y.H.; Yang, T. A visual peroxidase mimicking aptasensor based on Pt nanoparticles-loaded on iron metal organic gel for fumonisin B1 analysis in corn meal. *Biosens. Bioelectron.* **2022**, *209*, 114241. [[CrossRef](#)]
31. Zhang, L.; Du, X.; Su, Y.; Niu, S.; Li, Y.; Liang, X.; Luo, H. Quantitative assessment of AD markers using naked eyes: Point-of-care testing with paper-based lateral flow immunoassay. *J. Nanobiotechnol.* **2021**, *19*, 366. [[CrossRef](#)] [[PubMed](#)]
32. Chen, Y.; Ren, J.; Yin, X.; Li, Y.; Shu, R.; Wang, J.; Zhang, D. Vanadium Disulfide Nanosheet Boosts Optical Signal Brightness as a Superior Enzyme Label to Improve the Sensitivity of Lateral Flow Immunoassay. *Anal. Chem.* **2022**, *94*, 8693–8703. [[CrossRef](#)] [[PubMed](#)]
33. Wu, H.; Liu, J.; Chen, Z.; Lin, P.; Ou, W.; Wang, Z.; Xiao, W.; Chen, Y.; Cao, D. Mechanism and Application of Surface-Charged Ferrite Nanozyme-Based Biosensor toward Colorimetric Detection of l-Cysteine. *Langmuir* **2022**, *38*, 8266–8279. [[CrossRef](#)] [[PubMed](#)]

Disclaimer/Publisher's Note: The statements, opinions and data contained in all publications are solely those of the individual author(s) and contributor(s) and not of MDPI and/or the editor(s). MDPI and/or the editor(s) disclaim responsibility for any injury to people or property resulting from any ideas, methods, instructions or products referred to in the content.